Polymer 51 (2010) 3023–3030

Contents lists available at ScienceDirect

Polymer

journal homepage: www.elsevier.com/locate/polymer

Effect of 4-sulfobenzoic acid monopotassium salt on oligoanilines for inducing polyaniline nanostructures

Jun Kyu Park [1], Sang Soo Jeon [1], Seung Soon Im*

Department of Fiber and Polymer Engineering, Hanyang University, 17 Haengdang-dong, Seoul 133-791, Republic of Korea

ARTICLE INFO

Article history:
Received 11 March 2010
Received in revised form
30 April 2010
Accepted 4 May 2010
Available online 11 May 2010

Keywords:
Conducting polymer
Polyaniline nanotube
Oligoaniline

ABSTRACT

Polyaniline (PANI) nanotubes were chemically synthesized with the introduction of 4-sulfobenzoic acid monopotassium salt (KSBA) into an aqueous solution. As opposed to PANI microplates synthesized in the absence of KSBA, the PANI polymerized with KSBA exhibited tubular morphology, tens of micrometers long, with a total diameter of 130–240 nm, an inner diameter of 10–100 nm, and a wall thickness of 60–70 nm. The formation yield of PANI nanotubes was as high as about 95%, and the electrical conductivity was 4.8×10^{-1} S cm^{-1}. However, the PANI microplates exhibited about 10 times lower electrical conductivity of 3.1×10^{-2} S cm^{-1} than PANI nanotubes. The morphologies of the final PANIs were greatly affected by the morphologies of the oligoanilines produced with or without KSBA in the early polymerization stage. In this study, KSBA was introduced to regulate the reactant pH and to control oligoaniline morphology (with KSBA: 1D long nanosheets, without KSBA: 2D microplates). Synthetic time-resolved morphology dynamics revealed that the oligoanilines play a key role as templates for the PANI nanosheets polymerized by anilinium cations. Finally, the nanosheets transform into long PANI nanotubes through conformational changes induced by the protonation of the PANI chains in a highly acidic medium. Interestingly, the final products are a simple mixture of pure PANI nanotubes and oligoaniline complexes composed of oligoanilines and aniline sulfate salts. Thus, the oligoaniline do not grow into the PANI chains but function only as templates for the 1D PANI formation.

1. Introduction

Recently, various applications of nanostructured conducting polymers have inspired the development of facile and practical methods for the synthesis of conducting polymer nanostructures [1–7]. In particular, much effort has been directed toward one-dimensional (1D) polyaniline (PANI) nanostructures (e.g., nanofibers and nanotubes) because of their easy preparation, enhanced electrical properties and higher surface area than those of their bulk counterparts. Recently, PANI nanofibers/tubes have been readily synthesized by rapidly mixed reactions of desired concentrations of an aqueous monomer solution and an oxidant solution without templates.

Although these templateless routes to produce 1D PANI are simple, their formation mechanism is very complicated. Much research has been performed to investigate the formations of PANI nanofibers and nanotubes. For synthesis of 1D PANI nanostructures, it has been proposed that complexes like micelles are formed through the acid–base reaction between basic aniline monomers and various acids, e.g., inorganic acids [8], sulfonic acids [9] and carboxylic acids [10], which function as soft templates. Until now, this micelle model has been adopted as a general understanding of the formation mechanism of 1D PANI. However, the mechanism can not be fully explained by this micelle model because the inner diameter of the PANI nanotubes is larger than those of the micelles produced via reaction of aniline and various acids [11]. Moreover, the PANI nanotubes were successfully synthesized even in the absence of acids [12].

Recently, several research groups have proposed that water-insoluble oligoanilines produced early in the polymerization of aniline in an aqueous medium can act as templates for 1D PANI formation [13–15]. According to these studies, the oligoanilines consisted of phenazine derivatives stacked on top of each other. Then, PANI chains extend from the oligoanilines and act as ordered nuclei, resulting in 1D PANIs. More recently, it was reported that PANI intermediates composed of phenazine-like units and *para*-linked aniline units formed PANI nanotubes through self-curling behavior [16,17]. Based on the previously published papers, oligoanilines formed in the early stage of aniline polymerization seem to play a key role in the fabrication of 1D PANIs. Although much progress has been made in comprehending the formation of 1D PANIs, the overall mechanisms governing elongational growth and

* Corresponding author. Tel.: +82 2 2220 0495; fax: +82 2 2297 5859.
E-mail address: imss007@hanyang.ac.kr (S.S. Im).
[1] These authors contributed equally to this work.

0032-3861/$ – see front matter © 2010 Elsevier Ltd. All rights reserved.
doi:10.1016/j.polymer.2010.05.003

the factors determining the tubular or fibrous form of the PANIs are not yet clearly understood.

Here we report on a successful synthesis of PANI with highly uniform dimensions and a tubular morphology tens of micrometers long using a rolling mechanism at high aniline concentration (0.15 M). In particular, we found that the morphologies of the oligoanilines produced with 4-sulfobenzoic acid monopotassium salt (KSBA) in early stage polymerization were different from those produced in the absence of KSBA. Moreover, the morphologies of the final PANIs were greatly affected by the morphologies of the oligoanilines produced with or without KSBA. KSBA was firstly introduced to regulate the reactant pH, control oligoaniline morphology, and then produce PANI nanotubes tens of micrometer-long with total diameters of 130–240 nm. In order to investigate the formation mechanism of the 1D PANI nanostructures, synthetic time-resolved morphology dynamics using optical microscopy (OM) and scanning electron microscopy (SEM) were performed.

2. Experimental

2.1. Materials

Aniline (Sigma–Aldrich, 99.9%) was vacuum-distilled prior to use. Ammonium persulfate (APS) (Sigma–Aldrich) and 4-sulfobenzoic acid monopotassium salt (KSBA) (Sigma–Aldrich) were used as received without further purification.

2.2. Synthesis

Aniline (0.015 mol) and KSBA with different molar ratios were dissolved in 100 mL deionized water and were stirred at room temperature for 1 h. The ratios of [KSBA]/[An] were 0, 0.5, 1 and 2 in the different experiments. An aqueous APS (0.015 mol) solution (10 mL) was quickly poured into the above solution, and the reactant was left unperturbed. After 6 h, precipitated PANI samples were filtered and washed with distilled water and methanol several times, and then dried in a vacuum oven at 60 °C for 24 h.

2.3. Characterization

The acidities of the reaction mixtures were recorded in real-time using a digital pH-meter (HANNA Instruments, pH213 Microprocessor pH-meter). As soon as the polymerization began, a drop of reaction mixture was quickly deposited onto a glass slide. The morphological growth of oligoanilines in the initial stage of the polymerization was thereby observed using an optical microscope (OM) (Olympus, BX-51 TX) equipped with a CCD camera. In addition, the synthetic time-resolved morphological changes from oligoaniline to the final PANI nanostructures were observed using scanning electron microscopy (SEM) (JEOL, JSM6340) and transmission electron microscopy (TEM) (JEOL 2010). Fourier transform infrared (FT-IR) spectra were recorded on a PerkinElmer Spectrum 100 FT-IR spectrometer. Wide angle X-ray diffraction (WAXD) measurements were carried out on a Rigaku Denki X-ray generator (D/MAX-2500) using CuKα (λ = 1.5418 Å) radiation operated at 40 kV and 100 mA. The electrical conductivity (298 K) of a compressed pellet of the thoroughly washed and dried PANI samples was measured by the four-point microprobe method using a Jandel contact probe connected to a Keithley 238 high-current source measure unit. The electrical conductivity data were measured from three independent samples of a single synthesis.

3. Results and discussion

3.1. Morphological and structural characterization of PANI

Fig. 1 shows SEM images of the PANI samples synthesized with different concentrations of KSBA. The PANIs synthesized in the

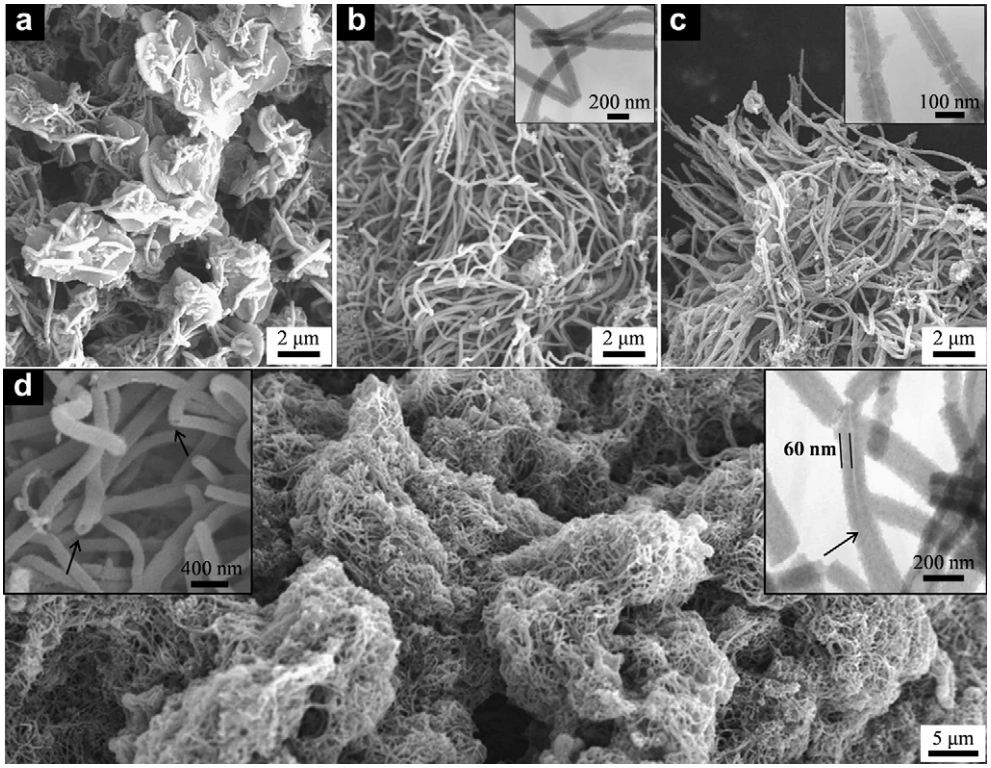

Fig. 1. SEM and TEM images of PANI synthesized at different [KSBA]/[An] ratios: a) 0, b) 0.5, c) 2 and d) 1. The left inset in d) shows a magnified SEM image. The arrows indicate the evidence of tubular morphology. The arrow in the right inset of d) indicates a semi-rolled PANI nanotube.

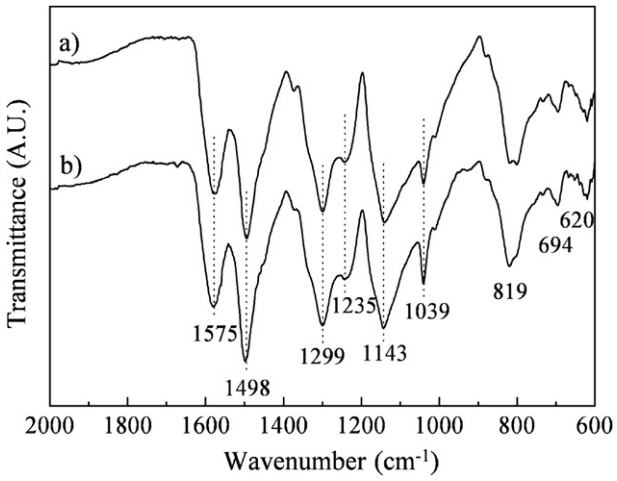

Fig. 2. FT-IR spectra of PANI samples synthesized at different [KSBA]/[An] ratios: a) 0 and b) 1.

absence of KSBA chiefly show 2D microplates with some extent of short nanofibers (Fig. 1a), analogous to previous reports using a template-free method with high aniline concentration (>0.1 M) [12,13,18]. However, different from the previous reports, PANIs with very long tubular morphologies are obtained independent of KSBA concentration when KSBA was introduced to the polymerization solution (Fig. 1b–d and inset TEM images). The lengths of the PANI nanotubes were several tens of micrometers, and the formation yield was about 95%, although they were synthesized at relatively higher monomer concentration and larger scale than other works [12,13,18]. PANI nanotubes had an outer diameter of 130–240 nm, an inner diameter of 10–100 nm, and a wall thickness of 60–70 nm (from Fig. 1b–d, inset TEM images). More interestingly, semi-rolled PANI nanotubes were observed in the TEM image of Fig. 1d. The morphological differences in the final PANIs (Fig. 1) appear to be affected by the addition of KSBA.

Although the morphologies of the PANIs are different from each other depending on the synthetic conditions, the FT-IR spectra of the PANIs show very similar characteristic peaks (Fig. 2). The C=C stretching deformations of the quinoid (1575 cm^{-1}) and benzenoid ring (1498 cm^{-1}), the C–N stretching of the secondary aromatic amine (1299 cm^{-1}), the aromatic C–H in-plane bending (1143 cm^{-1}), and the out-of-plane deformation of C–H bending in the 1,4-disubstituted benzene ring (819 cm^{-1}) are all observed

Table 1
Properties of PANI samples obtained at different [KSBA]/[An] ratios.

[KSBA]/[An]	Initial pH	Final pH	σ (S cm^{-1})	Morphology
0	7.5	1.2	3.1×10^{-2}	Microplates
0.5	4.9	1.1	1.2×10^{-1}	Nanotubes
1	4.5	1.1	2.6×10^{-1}	Nanotubes
2	3.6	1.1	4.8×10^{-1}	Nanotubes

[19,20]. The stretching vibrations of the SO_3^- group (1039, 694, and 620 cm^{-1}) [21–23] were also observed in all samples, indicating that the HSO_4^- anions created from APS or sulfonate anions of KSBA were incorporated into the main chain of the PANI samples as dopants. The existence of KSBA or hydrogen sulfate anions in doped PANI can be explained by proton dissociation from strong acids (e.g., $HOOCC_6H_4SO_3^-K^+ \rightarrow HOOCC_6H_4SO_3H \rightarrow HOOCC_6H_4SO_3^- + H^+$ and $H_2SO_4 \rightarrow HSO_4^- + H^+$) during the polymerization. Thus, the reaction mixture becomes more and more acidic as the polymerization proceeds.

3.2. Oxidative polymerization of aniline

The pH values of the reactants were recorded in real-time and decreased with increasing polymerization time, as shown in Fig. 3. During PANI polymerization, the pH value decreases due to the protons released from the monomers together with the protons dissociated from strong acids such as KSBA and sulfuric acid. As shown in Table 1, although the initial pH values of the polymerization solution with increasing [KSBA]/[An] ratio (=0, 0.5, 1 and 2) were 7.5, 4.9, 4.5 and 3.6, respectively, all of the final pH values were approximately 1.1–1.2. In addition, we observed that, with increasing KSBA concentration, the electrical conductivity of the final PANI increased (0.03 → 0.48 S cm^{-1}) and the morphology changed from plate-like to tubular form (Table 1). The electrical conductivity data of the PANI nanotubes synthesized in the presence of the KSBA were similar to the previous reports [9–12,14]. From our experimental results and those of previously published papers [12–17,24], the acidity profiles of the reaction can be divided into two reaction steps on the basis of pH ≈ 2.6. Aniline molecules seems to exist mainly as neutral molecules at pH > 2.6 where they produce oligoanilines through oxidation by APS [14,24]. However, aniline molecules in strong acidic solution, pH < 2.6, become protonated and convert to anilinium cations, which can easily be polymerized to PANI [14,24]. The oxidative polymerization of aniline without KSBA showed a sudden drop in pH within a short induction period, the time to reach the

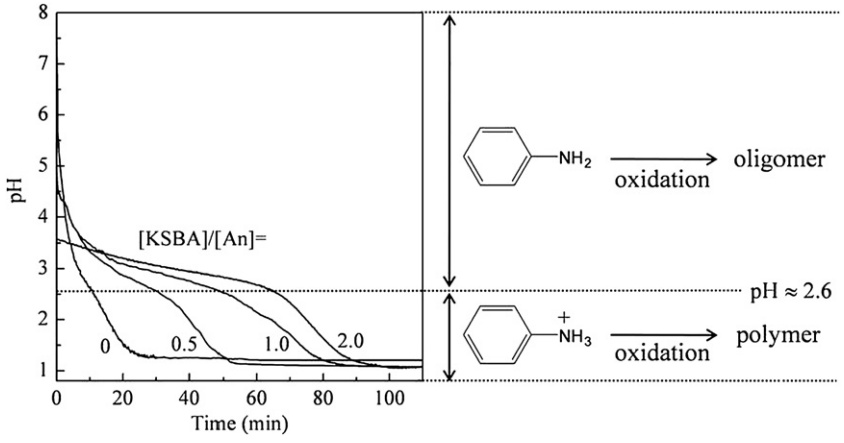

Fig. 3. Acidity profiles during the oxidation of 0.15 M aniline with 0.15 M APS at different [KSBA]/[An] ratios.

inflection point around pH ≈ 2.6. However, as the concentration of the KSBA in the polymerization solution increased, the induction period increased to a polymerization time of 65 min. The retardation in pH drop with increasing KSBA concentration can be ascribed to the steric hindrance of bulky KSBA molecules and the decrease in oxidation activity by a formation of a complex between K^+ ions from the KSBA and sulfate ions dissociated from APS. This is similar to the retardation of propagation by complex formation between cations of metal salts and sulfate ions in persulfate redox systems [25].

Fig. 4 shows the acidity and yield profiles of total product containing oligoaniline and pure PANI with increasing polymerization time. The oligoaniline is easily separated from the product owing to the methanol solubility of oligoaniline. The yields of oligoaniline and pure PANI were estimated based on the dry weight of the methanol-insoluble product (PANI) and the methanol-soluble product (oligoaniline). As can be seen in Fig. 4c, pure PANI is initially produced at a polymerization time of 50 min, and then the yield gradually increases. On the other hand, the yield of oligoaniline (%yield of total product − %yield of pure PANI) increases up to 50 min and then is constantly maintained at about 22% up to 150 min. Thus, the synthesis of the oligoanilines continues up to 50 min (pH > 2.6), after which, there seems to only be an increase in PANI produced at pH < 2.6. This yield data is in good accord with the above real-time pH result (Fig. 3). Therefore, the oligoanilines produced in the early polymerization stage (pH > 2.6) may not react with other aniline molecules to grow into the PANI chains, but exist until the final stage.

Indeed, based on our experimental results, the oligoanilines produced during the extended induction period seem to have a great effect on the morphologies of the final PANIs. Together with the above mentioned results, the morphological observations of the oligoanilines can provide clues for investigating the formation mechanism of the PANI nanostructures. The synthetic time-resolved morphological dynamics of the oligoanilines and final PANI will be discussed in detail below.

3.3. The morphological and structural analyses of oligoanilines

The growth mechanism of oligoanilines produced in the early polymerization stage in the presence of the KSBA was studied by optical microscopy (Fig. 5). On reaction initiation by APS, the oligoaniline seeds can be seen at $t = 15$ s. As reaction time increases up to $t = 60$ s, dendritic growth of oligoanilines from the seed is observed with sizes of several micrometers. On the other hand, the morphology of the oligoanilines produced without KSBA exhibited a bulky particulate morphology in the micrometer size range (data not shown).

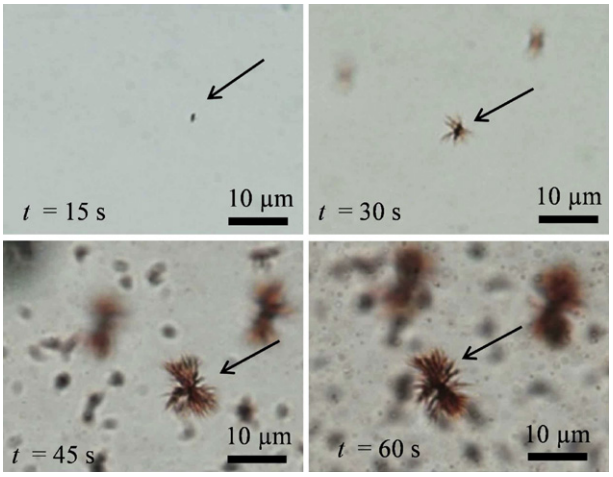

Fig. 5. Sequential OM images of the oligoanilines synthesized in 0.15 M KSBA solution at a given reaction time t (sec). The arrows indicate the dendritic growth of oligoaniline.

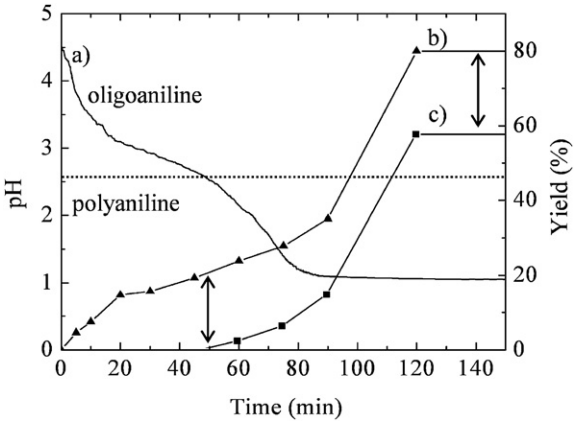

Fig. 4. Acidity and yield profiles during the oxidation of 0.15 M aniline with 0.15 M APS in 0.15 M KSBA solution. a) pH, b) total product yield and c) pure PANI yield.

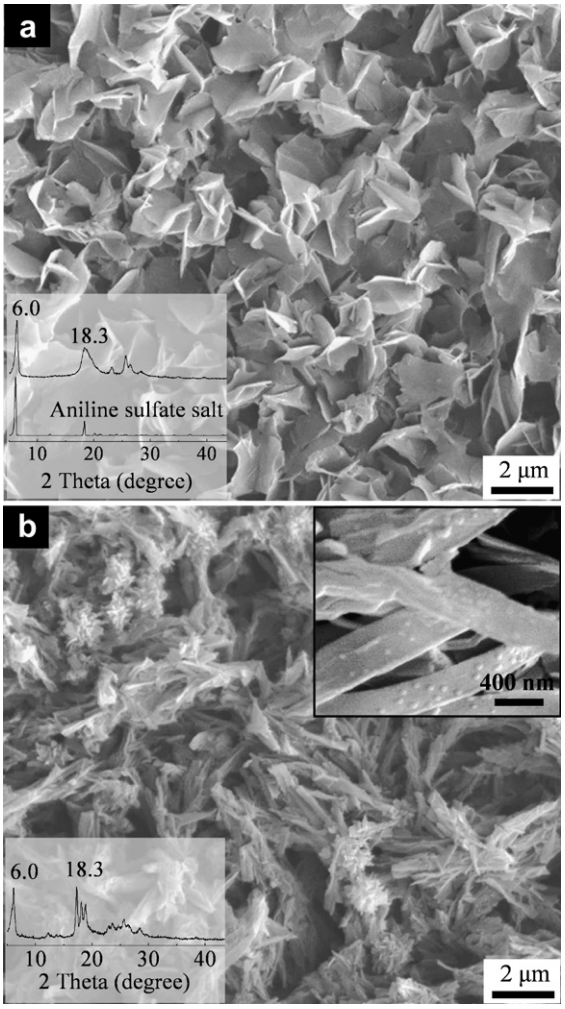

Fig. 6. SEM images and XRD patterns of oligoanilines produced at polymerization time $t = 5$ min at different [KSBA]/[An] ratios: a) 0 and b) 1. The inset in b) shows the magnified nanosheets of oligoaniline.

For longer polymerization times, $t = 5$ min, the morphological and structural differences in oligoanilines are shown in SEM images and XRD patterns in Fig. 6. The shape of the oligoanilines synthesized without KSBA exhibited 2D microplates (Fig. 6a), similar to that of the final PANI (Fig. 1a). However, the oligoanilines produced with KSBA possess a dendritic structure with branches of ribbon-like nanosheets tens of micrometers in length (Fig. 6b and inset). The oligoanilines with these peculiar morphologies are likely to play a role as seeds for final PANI growth.

The inset XRD patterns also show the structural differences between oligoanilines produced at $t = 5$ min. To compare with the oligoanilines produced under various synthetic conditions, XRD patterns of aniline sulfate salt precipitated by an acid–base reaction with aniline monomer and sulfuric acid are also provided. The XRD pattern of aniline sulfate salt shows a highly crystalline structure composed of two distinct peaks at around $2\theta = 6.0^\circ$ and 18.3°. Although all of the samples exhibited highly crystalline structures, the XRD pattern of the oligoaniline produced with KSBA was different from that of the oligoaniline produced without KSBA. This result may be related to the morphological differences in the oligoanilines. However, these two XRD patterns apparently have two peaks at around $2\theta = 6.0^\circ$ and 18.3°, similar to the characteristic peaks of the aniline sulfate salt. Thus, oligoanilines are apparently a complicated salt complex composed of aniline sulfate salts and other oligomers. Because of these complexations and the mixed structures of oligoanilines, accurate structure determination of oligoanilines has yet to be sufficiently clarified.

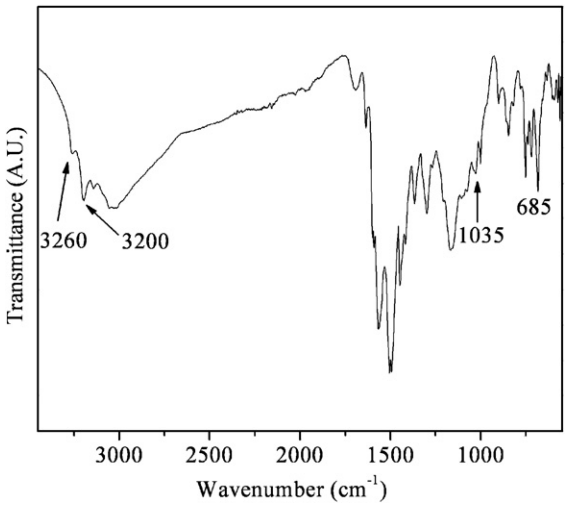

Fig. 7. FT-IR spectrum of oligoaniline obtained at polymerization time $t = 5$ min in 0.15 M KSBA solution.

The FT-IR spectrum of the oligoaniline obtained at a polymerization time of $t = 5$ min confirmed the existence of the sulfate

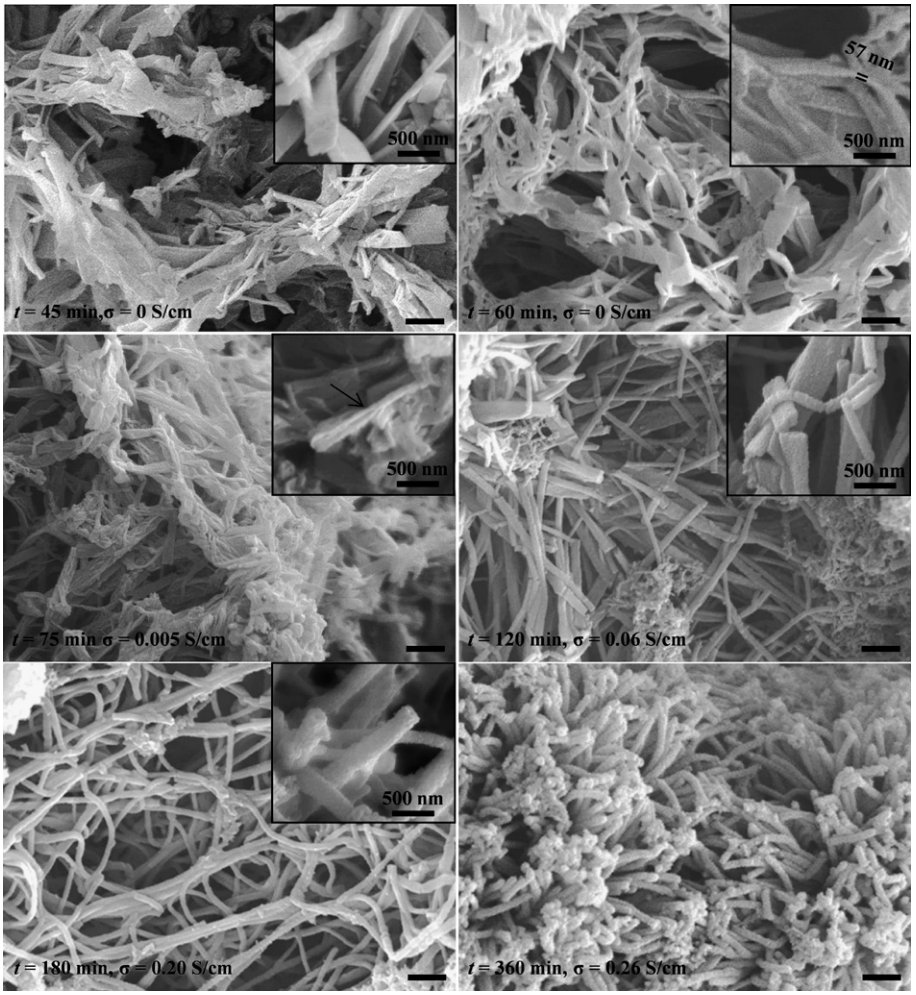

Fig. 8. Sequential SEM images showing the evolution of the PANI nanotubes produced in 0.15 M KSBA solution. The polymerization time and electrical conductivity are indicated in each image. The insets in $t = 45$–180 min show the magnified images. Scale bar: 1 μm.

group in oligoaniline (Fig. 7). This sulfate group can be identified by peaks at 1035, 685 and 619 cm^{-1} [21–23]. Moreover, the peaks at 3260 and 3200 cm^{-1} are assigned to the intra- and intermolecular hydrogen-bonded N–H stretching vibrations of the amine group (N–H … N or N–H … O), respectively [20,26,27]. Therefore, oligoanilines produced with KSBA possess crystalline structures through hydrogen bonding between oligoanilines and aniline sulfate salts.

3.4. Shape evolution of PANI nanotubes

Synthetic time-resolved SEM studies confirmed the shape evolution of PANI nanotubes produced in the presence of KSBA (Fig. 8). After adding APS, the oligoaniline nanosheets were continuously observed for up to $t = 45$ min (Fig. 8, $t = 45$ min). As the pH value decreases to around 2.6, flexible PANI nanosheets are gradually synthesized (Fig. 8, $t = 60$ min). Moreover, preexisting oligoaniline nanosheets may function as templates leading to the growth of PANI nanosheets. Although, it is difficult to distinguish clearly PANI nanosheets from preexisting oligoaniline nanosheets because of low yield of PANI as shown in Fig. 4, it is reasonable to assume that PANI nanosheets at this stage will be formed on the surfaces of oligoaniline nanosheets because residual aniline monomers can not only interact with the surfaces of oligoaniline nanosheets composed of aniline sulfate salts and phenazine-like units through hydrogen bonding and relatively strong $\pi-\pi$ interaction among aromatic rings but react with many active end groups such as =NH and $-NH_2$ of the surfaces of oligoaniline nanosheets. In addition, it is observed that the morphology of the nanosheets change from rigid form to flexible form at polymerization time of 45–75 min, as the PANI nanosheets are gradually produced. The PANI nanosheets synthesized prior to this stage are thought to have an emeraldine base form because they are electrically non-conducting.

As polymerization proceeds for up to 75 min, the PANI nanosheets begin to roll up (Fig. 8, $t = 75$ min, inset and Fig. 9a and b). The PANI chains at this stage may undergo a conformational change from an emeraldine base to an emeraldine salt by protonation in the highly acidic polymerization medium [28,29]. This conformational change in the PANI chains can further induce torsional movement within the chains, [30] which acts as a driving force for rolling the PANI nanosheets. Evidence for the protonation of PANI chains is provided by an increase in conductivity up to 0.005 S/cm. For further increasing polymerization time, PANI structures change into tubular forms (Fig. 8, $t = 120–180$ min) as a result of this rolling process. As a consequence of further polymerization, PANI nanotubes with a high electrical conductivity of 0.26 S/cm and uniform dimensions are obtained (Fig. 8, $t = 360$ min). Fig. 9c shows evidence for the binding of the two edges of PANI nanosheets to construct PANI nanotubes through a rolling mechanism. For additional experimental evidence about structural change during the shape evolution of PANI nanotubes, XRD analysis was performed for different polymerization times (Fig. 10). As polymerization proceeds for up to 45 min, the XRD peaks of oligoanilines composed of aniline sulfate salts and other aniline oligomers of phenazine-like units are clearly observed, as already shown in Fig. 6. After prolonged polymerization ($t = 60$ min), XRD peaks of oligoanilines broadens progressively as amorphous PANIs are initially synthesized. The change of XRD pattern in this range ($t = 45–60$ min) is in good accord with the yield profiles of oligoanilines and PANIs in Fig. 4. For further increasing polymerization time ($t = 120–360$ min), the intensity of XRD peaks associated with crystalline structure of oligoanilines more and more decreases and the XRD patterns show broad scattering at the peaks $2\theta = 15–30^{\circ}$. Based on the yield profiles of oligoanilines and PANIs and synthetic time-resolved SEM studies, this is due to the relatively increased yield of amorphous PANI chains instead of as-prepared oligoanilines.

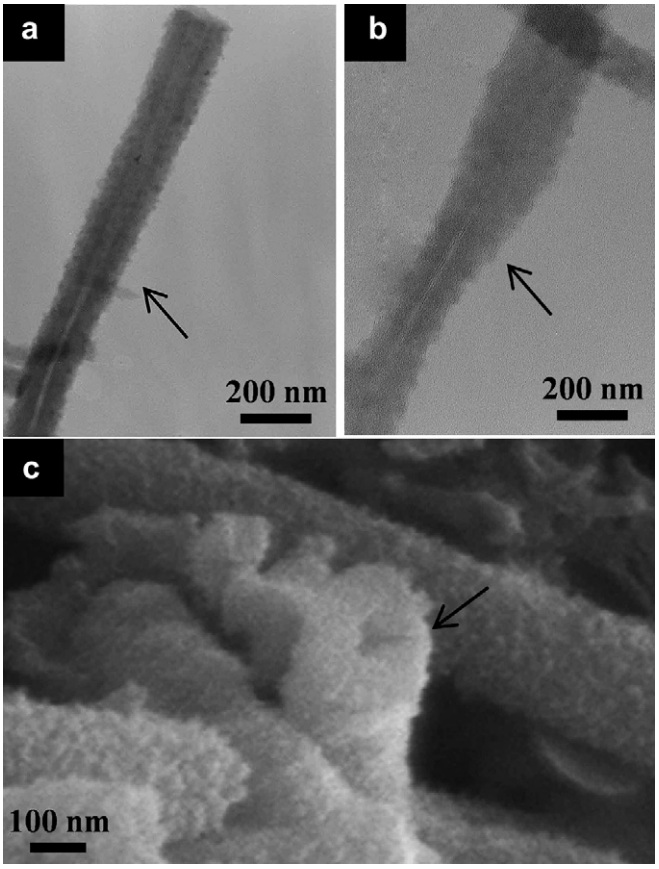

Fig. 9. a) and b) TEM images of semi-rolled PANI nanotubes obtained at polymerization time $t = 75$ min in 0.15 M KSBA solution. The arrows in a) and b) indicate semi-rolled PANI nanotubes. c) SEM image of a PANI nanotube obtained at polymerization time $t = 360$ min in 0.15 M KSBA solution. The arrow in c) indicates the commissure of the two edges of the PANI nanosheet.

The XRD patterns of the products obtained in the final stage ($t = 360$ min) are shown in Fig. 11. The final products contain both oligoanilines and pure PANI nanostructures (Fig. 11a), which can be

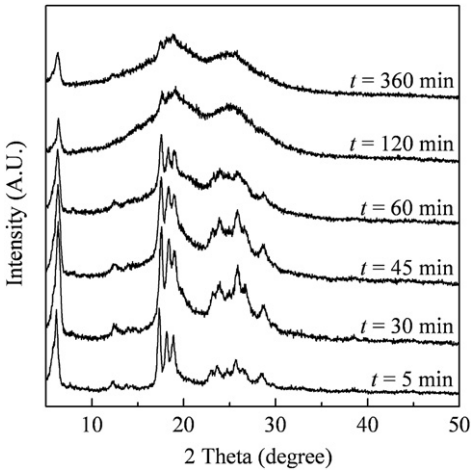

Fig. 10. XRD patterns of PANI nanotube formation in 0.15 M KSBA solution for different polymerization times. The samples used in XRD analysis were thoroughly washed with distilled water and dried before analysis.

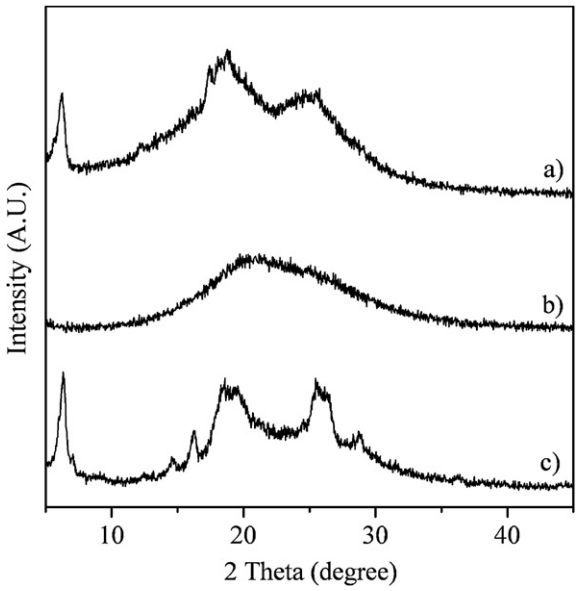

Fig. 11. XRD patterns of the products obtained in the final stage (t = 360 min). a) product washed with only water, b) pure PANI and c) recrystallized oligoaniline after methanol extraction.

separated by methanol filtering. After filtering, the methanol solution containing oligoanilines was dried, and then pure oligoanilines were recrystallized. The reported typical XRD patterns of chemically synthesized and doped PANI have two peaks centered at about $2\theta = 25.7$ and 20.4° ascribable to periodicities of perpendicular and parallel to the PANI chains, respectively [31,32]. However, the XRD pattern of our pure PANI (methanol-insoluble part) has a broad scattering amorphous structure (Fig. 11b). On the other hand, the XRD pattern (Fig. 11c) of oligoaniline extracted by methanol is similar to that of the oligoaniline produced at $t = 5$ min, as shown in Fig. 6. In addition, the tubular morphology of the pure PANI is not destroyed by removal of the oligoaniline through methanol washing, as shown in Fig. 1. Based on the above results, the final products are simple mixtures of pure PANI nanotubes and oligoaniline complexes composed of oligoanilines and aniline sulfate salts. Thus, the oligoaniline complexes produced in the early stages do not grow into the PANI chains, but function as only templates for 1D PANI formation. In addition, KSBA was introduced only to regulate the pH of reaction medium and to control oligoaniline morphology.

Fig. 12 illustrates the scheme of the rolling mechanism of PANI nanotubes synthesized in the presence of the KSBA: a) first, after adding APS, the oligoaniline nanosheets composed of aniline sulfate salts and oligomers of phenazine-like units are synthesized; b) oligoaniline nanosheets act like templates for the growth of PANI nanosheets of emeraldine base form; c) PANI nanosheets start to be rolled up by the conformational change due to the protonation of PANI chains under acidic condition; d) finally, PANI nanotubes are fabricated as a result of the rolling process.

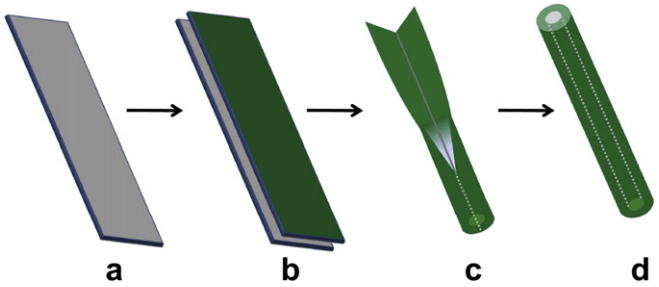

Fig. 12. Scheme of the rolling mechanism of PANI nanotubes. a) oligoaniline nanosheet, b) oligoaniline nanosheet and PANI nanosheet of emeraldine base form, c) semi-rolled PANI nanotube, and d) PANI nanotube.

4. Conclusions

Highly uniform and long PANI nanotubes with total diameters of 130–240 nm were easily synthesized in KSBA solution. The oligoanilines produced at pH > 2.6 possessed dendritic microstructures and were non-conducting. These oligoanilines acted as templates for further growth of PANI nanostructures. As the pH of the polymerization solution decreased below 2.6, the PANIs conglomerated into nanosheets with morphologies similar to that of oligoaniline. Finally, the nanosheets were transformed into PANI nanotubes through a rolling mechanism. The driving force of the rolling mechanism may be attributed to the conformational change via protonation of the PANI chains forming nanosheets in a highly acidic medium. Furthermore, the addition of KSBA regulated the pH drop of reaction medium and contributed to the fabrication of micrometer-long 1D PANIs. Although we have confirmed the preparation and formation mechanism of PANI nanotubes based on acidity control of polymerization medium via addition of KSBA, it is possible to control the PANI morphology using other pH-regulating additives to the reaction medium, including aniline monomer. In particular, our method to fabricate the PANI nanotubes discussed here can have advantages in mass production of high purity, because, although the PANI nanotubes were synthesized at relatively higher monomer concentration and larger scale than other works, they had a high formation yield of about 95%.

Acknowledgements

This work was supported by Basic Science Research Program through the National Research Foundation of Korea (NRF) grant funded from the Ministry of Education, Science and Technology (MEST) of Korea for the Center for Next Generation Dye-sensitized Solar Cells (No. 2010-0001842) and research fund of Hanyang Universitiy (HYU-2010-T).

References

[1] Choi JW, Han MG, Kim SY, Oh SG, Im SS. Synth Met 2004;141:293–9.
[2] Jang J, Oh JH. Adv Funct Mater 2005;15:494–502.
[3] Marinakos SM, Shultz DA, Feldheim DL. Adv Mater 1999;11:34–7.
[4] Chiou NR, Epstein AJ. Adv Mater 2005;17:1679–83.
[5] Huang JH, Kaner RB. Angew Chem 2004;116:5941–5.
[6] Wei Z, Zhang Z, Wan M. Langmuir 2002;18:917–21.
[7] Jeon SS, Park JK, Yoon CS, Im SS. Langmuir 2009;25:11420–4.
[8] Zhang Z, Wei Z, Wan M. Macromolecules 2002;35:5937–42.
[9] Zhang Z, Wei Z, Zhang L, Wan M. Acta Mater 2005;53:1373–9.
[10] Zhang L, Long Y, Chen Z, Wan M. Adv Funct Mater 2004;14:693–8.
[11] Konyushenko EN, Stejskal J, Sedenková I, Trchová M, Sapurina I, Cieslar M, et al. Polym Int 2006;55:31–9.
[12] Ding H, Shen J, Wan M, Chen Z. Macromol Chem Phys 2008;209:864–71.
[13] Trchová M, Sedenkova I, Konyushenko EN, Stejskal J, Holler P, Ćirić-Marjanović G. J Phys Chem B 2006;110:9461–8.
[14] Stejskal J, Sapurina S, Trchová M, Konyushenko EN, Holler P. Polymer 2006;47:8253–62.
[15] Kříž J, Starovoytova L, Trchová M, Konyushenko EN, Stejskal J. J Phys Chem B 2009;113:6666–73.
[16] Huang YF, Lin CW. Polymer 2009;50:775–82.
[17] Huang YF, Lin CW. Synth Met 2009;159:1824–30.
[18] Chiou NR, Lee LJ, Epstein AJ. Chem Mater 2007;19:3589–91.
[19] Han MG, Cho SK, Oh SG, Im SS. Synth Met 2003;126:53–60.
[20] Sapurina I, Osadchev AY, Volchek BZ, Trchová M, Riede A, Stejskal J. Synth Met 2002;129:29–37.

[21] Janosevic A, Ćirić-Marjanović G, Marjanovic B, Holler P, Trchová P, Stejskal J. Nanotechnology 2008;19:135606–13.
[22] Lü QF, Huang MR, Li XG. Chem Eur J 2007;13:6009–18.
[23] Li XG, Hou ZZ, Huang MR, Moloney MG. J Phys Chem C 2009;113:21586–95.
[24] Stejskal J, Sapurina I, Trchová M, Konyushenko EN. Macromolecules 2008;41:3530–6.
[25] Sarac AS. Prog Polym Sci 1999;24:1149–204.
[26] Kieffel Y, Travers JP, Ermolieff A, Rouchon D. J Appl Polym Sci 2002;86:395–404.
[27] Zheng W, Angelopoulos M, Epstein AJ, MacDiarmid AG. Macromolecules 1997;30:2953–5.
[28] Wang Z, Zhou S, Wu L. Adv Funct Mater 2007;17:1790–4.
[29] Laska J. J Mol Struct 2004;701:13–8.
[30] Colomban P, Folch S, Gruger A. Macromolecules 1999;32:3080–92.
[31] Li XG, Lü QF, Huang MR. Small 2008;4:1201–9.
[32] Li XG, Li A, Huang MR. Chem Eur J 2008;14:10309–17.